A Journal of the Gesellschaft Deutscher Chemiker

Angewandte International Edition Chemie

GDCh

www.angewandte.org

Accepted Article

Title: Photon-induced near-field electron microscopy (PINEM) of eukaryotic cells

Authors: Mohammed Kaplan, Byung-Kuk Yoo, Jau Tang, Tony Karam, Bolin Liao, Devdoot Majumdar, david Baltimore, Grant Jensen, and Ahmed Zewail

To be cited as: *Angew. Chem. Int. Ed.* 10.1002/anie.201706120
Angew. Chem. 10.1002/ange.201706120

Link to VoR: http://dx.doi.org/10.1002/anie.201706120
http://dx.doi.org/10.1002/ange.201706120

WILEY-VCH

10.1002/anie.201706120

WILEY-VCH

COMMUNICATION

Photon-induced near-field electron microscopy (PINEM) of eukaryotic cells

Mohammed Kaplan[a], Byung-Kuk Yoo[a], Jau Tang[a]*, Tony E. Karam[a], Bolin Liao[a], Devdoot Majumdar[b], David Baltimore[b], Grant J. Jensen[c]* & Ahmed H. Zewail[a]†

Abstract: Photon-induced near-field electron microscopy (PINEM) is a technique to produce and then image evanescent electromagnetic fields on the surfaces of nanostructures. Most previous applications of PINEM have imaged surface plasmon-polariton waves on conducting nanomaterials. Here, the application of PINEM on whole human cancer cells and membrane vesicles isolated from them is reported. We show that photons induce time-, orientation-, and polarization-dependent evanescent fields on the surfaces of A431 cancer cells and isolated membrane vesicles. Furthermore, the addition of a ligand to the major surface receptor on these cells and vesicles (Epidermal Growth Factor Receptor, EGFR) reduces the intensity of these fields in both preparations. In the absence of plasmon waves in biological samples, we propose these evanescent fields reflect the changes of EGFR kinase domain polarization upon ligand binding.

Because electrons can be accelerated until their wavelengths are much smaller than an Angstrom, electron microscopes have been able to deliver spatial information about a wide variety of materials at atomic resolution. The development of Ultrafast Electron Microscopy (UEM) has now added atomic-scale time resolution (femtosecond) as well, providing new insights into dynamics (See Ref. [1,2] and references therein). UEM achieves this by combining the transmission electron microscope (TEM) with two femtosecond laser pulses [3]. The first pulse (the "pump," or clocking pulse) is directed to the sample, where it induces dynamic changes. The second, "probe" pulse irradiates the TEM cathode to generate an electron (the "electron" pulse), which is then accelerated and focused onto the sample a controllable number of femtoseconds after the pump pulse. Images are built up by many millions of pump-probe events which each involve a single electron. Over the last decade, UEM has been used to study the structure and dynamics of materials using imaging, diffraction and electron-energy-loss-spectroscopy detection modes [4–10].

In the variation of UEM called photon-induced near-field electron microscopy (PINEM), the precise spatiotemporal overlap between the pump pulse and the electron pulse on the surface of a nanostructure leads to an electron-photon coupling between the imaging electron and the evanescent fields induced by the pump pulse on the nanostructure surface [11,12]. Due to the coupling, the electron can gain or lose energy in multiples of the photon quanta. By allowing only the electrons that gain energy to pass through the energy filter it is possible to visualize the dynamic evanescent electromagnetic fields created on the sample surface by the pump pulse. Although still in its infancy, PINEM has already been used for instance to study the quantum behavior of Rabi oscillations [13], the wave-particle duality of light [14], ultrashort electron packets [15,16], nanoparticle entanglement [17], dielectric properties [18,19], and the ultrafast dynamics of conducting nanomaterials [20]. Despite its wide applications in inorganic nanomaterials, the biological applications of PINEM have so far been limited to a single study on purified protein vesicles and *Escherichia coli* [21]. Photon-induced near fields were demonstrated on the aforementioned biological materials, but hitherto no physical explanations were offered for the effect in these materials, which lack conducting electrons.

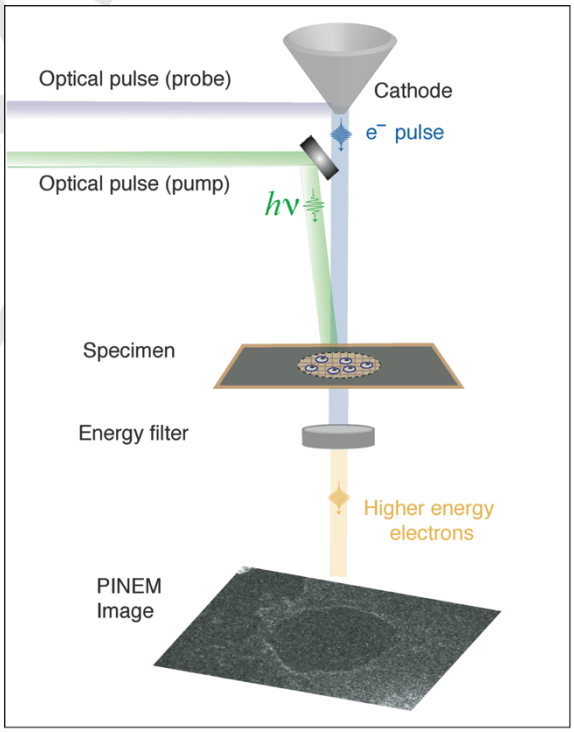

Figure 1: A schematic representation of the PINEM experiment. A femtosecond laser pulse (violet) is directed to the cathode and is used to generate single-electron pulses (blue). A second femtosecond laser pulse (green) is directed to the sample inside the microscope. When both the electrons and the photons arrive at the sample at the same time, some of the electrons gain or lose integers of the photon energy quanta. By removing all the electrons except those that gained energy, PINEM images can be produced.

Here, we explore the use of PINEM on human cancer cells, namely A431 cells, and membrane vesicles isolated from them and the effect of ligand binding on the electron-photon coupling on the edges of these cells and membrane vesicles. The A431 human cancer cells are known to have high expression levels of Epidermal Growth Factor Receptor (EGFR) on their

[a] M. Kaplan, BK YOO, J. Tang, T. Karam, B. Liao and A.H. Zewail,
Physical Biology Center for Ultrafast Science and Technology, Arthur Amos Noyes Laboratory of Chemical Physics, California Institute of Technology, Pasadena, California 91125, USA.
[b] D. Majumdar and D. Baltimore
Division of Biology and Biological Engineering, California Institute of Technology, Pasadena, CA.
[c] G. J. Jensen
California Institute of Technology, Pasadena, CA 91125, USA.
Howard Hughes Medical Institute, Pasadena, CA 91125, USA.
† Deceased on August 2nd, 2016.
* Jau Tang: Jautang@caltech.edu
Grant J. Jensen: Jensen@caltech.edu

10.1002/anie.201706120

WILEY-VCH

COMMUNICATION

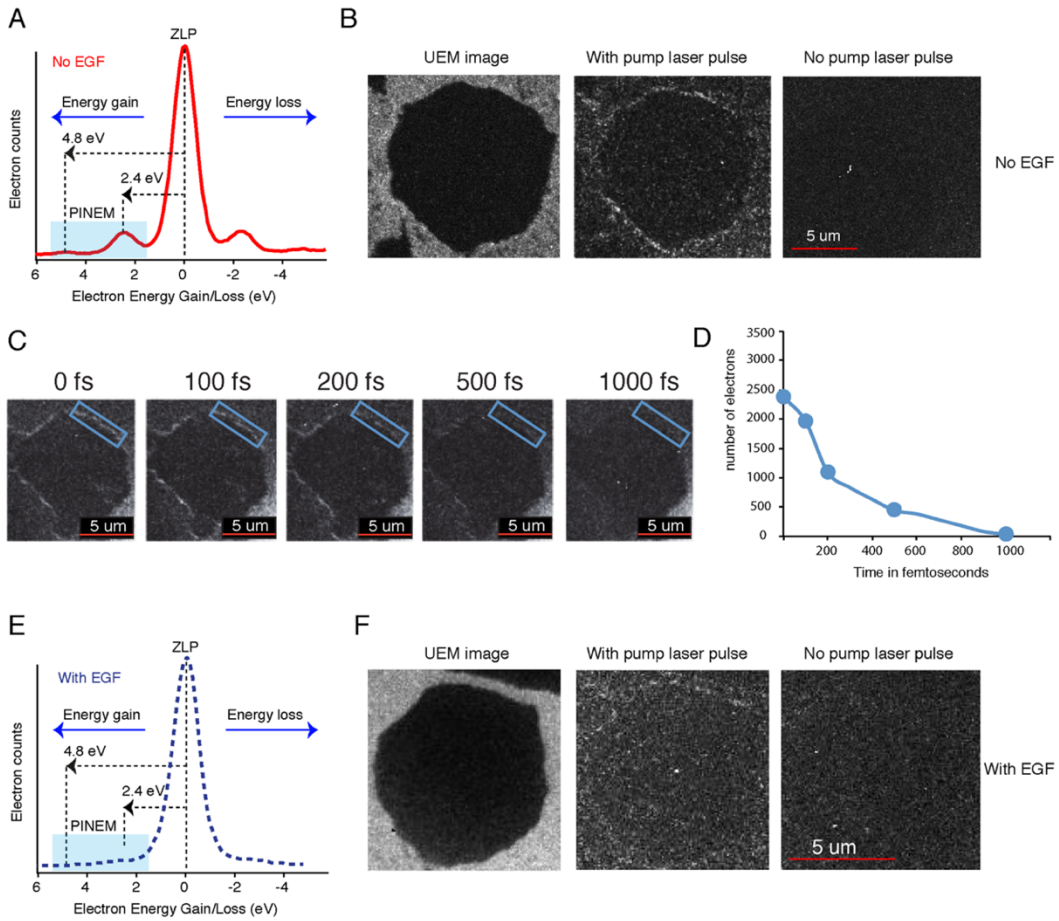

Figure 2: A) Electron energy spectrum of A431 cell without EGF. Electron energy gain equivalent to one and two photon quanta is indicated (2.4 eV and 4.8 eV). **B)** UEM (left) and PINEM images (middle and right) of A431 cells without EGF. Electron-photon coupling is manifest by the bright ring around the cell periphery. **C)** Time-dependency of electron-photon coupling as a function of the delay between the pump and the electron pulses on the cell surface. Time zero is defined as when there is maximum coupling. The intensity of PINEM images decreases as the time difference between the two pulses increases. After 1 picosecond (right image), almost no coupling is observed on the surface of the cell. **D)** A plot indicating the number of electrons arriving on the detector in the area highlighted by the blue box in C for each time point. **E)** Electron energy spectrum of A431 cell incubated with EGF. Electron energy gain equivalent to one and two photon quanta is indicated (2.4 eV and 4.8 eV). **F)** As in B but for cells incubated with EGF. The brightness of the ring around the cell (middle) is diminished as compared to panel B. These measurements were performed at room temperature. Scale bar is 5 µm.

surface (~ 2.5x10^6 receptors/cell) [22]. EGFR is a tyrosine kinase receptor involved in cell proliferation and division and is directly implicated in the development of many cancers [23]. The 1,286-amino-acid receptor consists of an extracellular domain (ECD), a transmembrane domain, a juxtamembrane domain, a kinase domain and an unstructured C-terminal tail. Upon binding to its ligand, the Epidermal Growth Factor (EGF), the receptor becomes phosphorylated and forms dimers on the cell surface [24]. Atomic models for isolated domains of EGFR are available from X-ray crystallography and NMR spectroscopy [25–28]. Recently, a NMR study provided insight into the dynamics and ligand-induced activation mechanism of the full-length EGFR in native membrane vesicles. [29]. Our results here demonstrate that femtosecond laser pulses induce the formation of electromagnetic fields that can couple to electrons on the surface of A431 cells. Moreover, we show that the intensity of this electron-photon coupling depends on the conformation of the abundant membrane protein, EGFR, on the cell surface. The addition of EGFR ligand to A431 cells reduces the intensity of the photon-electron coupling on the surface of whole cellular and vesicular preparations.

Figure 1 depicts the experimental setup used for our study. First, unfixed A431 cells were deposited on silicon oxide grids (see Materials and Methods) and left to dry. The samples were then imaged using the second generation UEM (UEM2) at Caltech [30]. The average diameter of A431 cells is between 15 - 25 µm and they are typically a few micrometers thick. At time zero (defined as producing the maximal coupling between the pump and the electron pulses) symmetrical peaks were observed in the electron energy spectrum to the left (gain region) and right (loss region) of the zero loss peak (ZLP) when the electron beam was confined to the cell surface (Figure S1A). To confirm that the observed coupling is occurring on the cell, a control experiment was performed by confining the electron beam to a cell-free area on the grid (Figure S1B). No peaks in the gain and loss regions of the electron energy spectra were observed.

By allowing only those electrons that gained energy via the electron-photon coupling to pass through the energy filter, images of the laser-induced ultrafast evanescent fields on the cells were produced (Figures 2A & B, middle image). As a further control, additional images were obtained in the absence of the pump pulse, and no fields were detected (Figure 2B, right image). This experiment was repeated three times on different samples and showed the same quantitative result (Figure S2). The nature of these fields and the PINEM approach were explored by characterizing the time-, orientation- and polarization-dependency of the electron-photon coupling on the cell surface. By altering the delay between the pump and the electron pulses on the cell, it was observed that the coupling decreases significantly after 200 fs and almost disappears after 1000 fs (Figures 2C & D). The temporal resolution of the experiment depends mainly on the overlap between the pump and electron pulses, which had durations of ~ 250 fs and 750 fs respectively.

Moreover, tilting the sample by different angles (+30º and -30º) lead to a change in the PINEM image, indicating that coupling also depends on the local orientation of the sample with respect to the beam (Figure S3). Finally, in accordance with previous PINEM experiments on biological and inorganic materials, the coupling also depends on the polarization of the pump pulse, with the highest intensity obtained when the polarization is perpendicular to the cell edge (Figure S4). In these experiments very low electron doses were used (0.3 e/A^2) [31,32], and no changes in the samples were detected "before" and "after" images and spectra.

As mentioned previously, A431 cells are known to express large numbers of EGF receptors on their membranes. Hence, the effect of EGF binding on the electron-photon coupling on the cell surface was examined. To test this, EGF was added to the cells to induce receptor dimerization (but not internalization, see Materials and Methods) and the experiment was repeated. The addition of EGF resulted in a significant decrease in the intensity of the loss and gain peaks in the spectrum (Figure 2E) indicating weaker electron-photon coupling on the cells surface. Images of A431 cells incubated with EGF showed correspondingly lower intensities (Figure 2F). This experiment was reproduced three times on different samples and yielded similar results (Figure S5). As a control, the experiment was repeated with aprotinin, a protein with the same size as EGF but that does not bind EGFR. Here, strong coupling was again observed compared to the EGF-bound cells (Figure S6), indicating that the decrease in intensity after the addition of EGF is due to its specific interaction with EGFR.

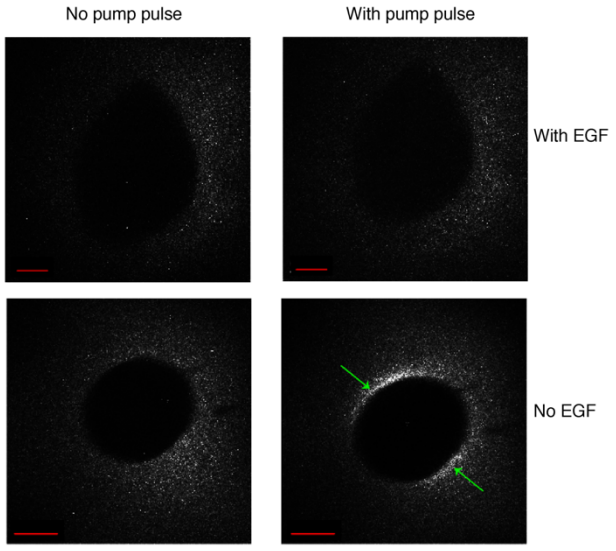

Figure 3: PINEM images of membrane vesicles isolated from A431 cells with (top row) and without EGF (bottom row). Left column indicates images without a pump pulse and right column indicates images taken in the presence of the pump pulse. Green arrows highlight the evanescent fields on the edges of the vesicle. These measurements were performed at low temperatures (Materials and Methods). Scale bar is 200 nm.

Recently, it was shown that membrane vesicles isolated from A431 cells are enriched with EGFR on their surface by a factor of 5.5 compared to whole cells with the receptor being still functional and capable of binding to its ligand [29]. For this reason, membrane vesicles were isolated from A431 cells and PINEM measurements on the vesicles with and without EGF were obtained (Materials and Methods). These vesicles had a diameter of a few hundred nanometers. Again, the addition of EGF to the vesicles resulted in weaker evanescent fields on their edges in a pattern similar to what was observed for whole cells (Figure 3). It has been proposed that the intensity of the photon-induced near field effect on the surface of materials is strongly dependent on the induced dipole moment formed on the surface by the pump pulse [12]. On the other hand, the magnitude of the induced dipole moment is directly proportional to the polarization of the material [33]. Previous studies showed that the kinase domain of the ligand-free inactive dimer is strongly polarized [34], and that 30- 40 % of EGFR adapts this conformation on the cell surface in the absence of EGF [35]. We hypothesize that the strongly polarized kinase domain of the inactive EGFR dimer compared to that of the ligand-bound dimer is responsible for the observed electron-photon coupling in the absence of EGF addition.

Some important biological processes in the cell occur at the femtosecond time scale, including for instance charge migration in the early stages of protein-ligand interactions, some enzyme catalytic processes and photon-capture events by photoreceptors like rhodopsin (See ref. [36,37]). The high-temporal-resolution of PINEM, especially with the development of shorter electron pulses [38], opens the door for further applications in the study of ultrafast biological events on the cell surface.

Experimental Section

Experimental Details and Supporting information are available on a separate file.

Acknowledgements

We thank Spencer Baskin and Mohammed Hassan for helpful discussions. This work was supported by the National Science Foundation Grant DMR-0964886 and the Air Force Office of Scientific Research Grant FA9550-11-1-0055 for research conducted in The Gordon and Betty Moore Center for Physical Biology at the California Institute of Technology.

Keywords: Ultrafast electron microscopy • Femtobiology • Photon-electron coupling • PINEM •

[1] A. H. Zewail, *Science.* **2010**, *328*, 187–193.
[2] G. M. Vanacore, A. W. P. Fitzpatrick, A. H. Zewail, *Nano Today* **2015**, *11*, 228–249.
[3] V. A. Lobastov, R. Srinivasan, A. H. Zewail, *Proc. Nat. Acad. Sci. USA* **2005**, *102*, 7069–7073.
[4] F. Carbone, O. H. Kwon, A. H. Zewail, *Science.* **2009**, *325*, 181–184.
[5] B. Barwick, H. Park, O. H. Kwon, J. S. Baskin, A. H. Zewail, *Science.* **2008**, *322*, 1227–1231.
[6] A. W. P. Fitzpatrick, U. J. Lorenz, G. M. Vanacore, A. H. Zewail, *J. Am. Chem. Soc.* **2013**, *135*, 19123–19126.
[7] O. H. Kwon, A. H. Zewail, *Science.* **2010**, *328*, 1668–1673.
[8] R. M. van der Veen, O. H. Kwon, A. Tissot, A. Hauser, A. H. Zewail, *Nat. Chem.* **2013**, *5*, 395–402.
[9] U. J. Lorenz, A. H. Zewail, *Proc. Nat. Acad. Sci. USA* **2013**, *110*, 2822–2827.

[10] O. F. Mohammed, P. C. Samartzis, A. H. Zewail, *J. Am. Chem. Soc.* **2009**, *131*, 16010–16011.
[11] B. Barwick, D. J. Flannigan, A. H. Zewail, *Nature* **2009**, *462*, 902–906.
[12] S. T. Park, M. Lin, A. H. Zewail, *New J. Phys.* **2010**, *12*, 123028.
[13] A. Feist, K. E. Echternkamp, J. Schauss, S. V Yalunin, S. Schäfer, C. Ropers, *Nature* **2015**, *521*, 200–203.
[14] L. Piazza, T. T. A. Lummen, E. Quiñonez, Y. Murooka, B. W. Reed, B. Barwick, F. Carbone, *Nat. Commun.* **2015**, *6*, 6407.
[15] D. A. Plemmons, S. Tae Park, A. H. Zewail, D. J. Flannigan, *Ultramicroscopy* **2014**, *146*, 97–102.
[16] F. O. Kirchner, A. Gliserin, F. Krausz, P. Baum, *Nat. Photonics* **2013**, *8*, 52–57.
[17] A. Yurtsever, J. S. Baskin, A. H. Zewail, *Nano Lett.* **2012**, *12*, 5027–5032.
[18] A. Yurtsever, R. M. van der Veen, A. H. Zewail, *Science.* **2012**, *335*, 59–64.
[19] T. T. A. Lummen, R. J. Lamb, G. Berruto, T. LaGrange, L. Dal Negro, F. J. García de Abajo, D. McGrouther, B. Barwick, F. Carbone, *Nat. Commun.* **2016**, *7*, 13156.
[20] M. T. Hassan, H. Liu, J. S. Baskin, A. H. Zewail, *Proc. Nat. Acad. Sci. USA* **2015**, *112*, 12944–12949.
[21] D. J. Flannigan, B. Barwick, A. H. Zewail, **2010**, *107*, *Proc. Nat. Acad. Sci. USA* **2010**, *107*, 9933-9937.
[22] H. Haigler, J. F. Ash, S. J. Singer, S. Cohen, *Proc. Nat. Acad. Sci. USA* **1978**, *75*, 3317–3321.
[23] C. L. Arteaga, J. A. Engelman, *Cancer Cell* **2014**, *25*, 282–303.
[24] P. Winckler, L. Lartigue, G. Giannone, F. De Giorgi, F. Ichas, J. B. Sibarita, B. Lounis, L. Cognet, *Sci. Rep.* **2013**, *3*, 2387.
[25] K. M. Ferguson, M. B. Berger, J. M. Mendrola, H. S. Cho, D. J. Leahy, M. A. Lemmon, *Mol. Cell* **2003**, *11*, 507–517.
[26] H. Ogiso, R. Ishitani, O. Nureki, S. Fukai, M. Yamanaka, J. H. Kim, K. Saito, A. Sakamoto, M. Inoue, M. Shirouzu, et al., *Cell* **2002**, *110*, 775–787.
[27] J. Stamos, M. X. Sliwkowski, C. Eigenbrot, *J. Biol. Chem.* **2002**, *277*, 46265–46272.
[28] N. F. Endres, R. Das, A. W. Smith, A. Arkhipov, E. Kovacs, Y. Huang, J. G. Pelton, Y. Shan, D. E. Shaw, D. E. Wemmer, et al., *Cell* **2013**, *152*, 543–556.
[29] M. Kaplan, S. Narasimhan, C. de Heus, D. Mance, S. van Doorn, K. Houben, D. Popov-Čeleketić, R. Damman, E. A. Katrukha, P. Jain, et al., *Cell* **2016**, *167*, 1241–1251.
[30] H. S. Park, J. S. Baskin, O. H. Kwon, A. H. Zewail, *Nano Lett.* **2007**, *7*, 2545–2551.
[31] C. V Iancu, E. R. Wright, J. B. Heymann, G. J. Jensen, *J. Struct. Biol.* **2006**, *153*, 231–240.
[32] H. Stark, F. Zemlin, C. Boettcher, *Ultramicroscopy* **1996**, *63*, 75–79.
[33] H. J. C. Berendsen, J. R. Grigera, T. P. Straatsma, *J. Phys. Chem.* **1987**, *91*, 6269–6271.
[34] N. Jura, N. F. Endres, K. Engel, S. Deindl, R. Das, M. H. Lamers, D. E. Wemmer, X. Zhang, J. Kuriyan, *Cell* **2009**, *137*, 1293–1307.
[35] E. G. Hofman, A. N. Bader, J. Voortman, D. J. Van Den Heuvel, S. Sigismund, A. J. Verkleij, H. C. Gerritsen, P. M. P. Van Bergen en Henegouwen, *J. Biol. Chem.* **2010**, *285*, 39481–39489.
[36] D. Zhong, *Curr. Opin. Chem. Biol.* **2007**, *11*, 174–181.
[37] V. Sundström, *Annu. Rev. Phys. Chem.* **2008**, *59*, 53–77.
[38] M. T. Hassan, J. S. Baskin, B. Liao, A. H. Zewail, *Nat. Photonics* **2017**, 11, 425–430.

10.1002/anie.201706120

WILEY-VCH

COMMUNICATION

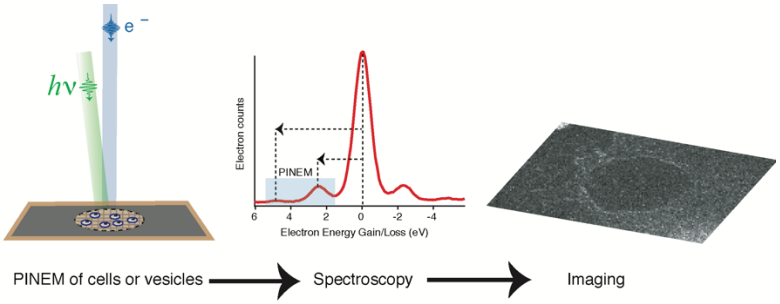

Caught in the act
Accurate synchronization of femtosecond laser and electron pulses in an electron microscope allows the formation and visualization of electromagnetic fields on the surface of eukaryotic cells. These fields are in the femtosecond timescale and are sensitive to the conformational changes in the membrane proteins on the cell surface.